Auger energies of free atoms: Comparison between experiment and relativistic theory

H. Aksela, S. Aksela, and H. Patana
Department of Physics, University of Oulu, Linnanmaa, SF-90570 Oulu 57, Finland
(Recieved 5 December 1983)

Kinetic energies of the Auger transitions are calculated with the multiconfiguration Dirac-Fock method for selected elements for which reliable experimental free-atom data are available. A critical comparison between calculated and experimental data is presented.

I. INTRODUCTION

A reliable comparison of atomic calculations with experimental Auger energies is only possible if the experimental values are measured from free atoms. During the last few years the number of free-atom spectra studied has considerably increased due to the numerous new high-temperature-vapor measurements. Thus a more systematic comparison between calculated and experimental kinetic energies now becomes possible. We restrict our comparisons to elements for which reliable experimental data exist in the usual energy region of the current free-atom measurements: 20—1500 eV. The elements studied are Ne, Na, Mg, Ar, K, Cu, Zn, Kr, Pd, Ag, Cd, In, Xe, Cs, Yb, Au, and Hg. The experimental energies presented in this report have mainly been taken from the literature; but some unpublished results obtained by our research group are also given. The previously published experimental Auger energies are now slightly corrected to correspond to the new energy calibration.

The theoretical calculations are carried out with the multiconfiguration Dirac-Fock program of Grant *et al.*[1,2] The energies of Auger transitions are obtained as differences between separately optimized total energies of the singly ionized initial- and doubly ionized final-state levels of the Auger process (the ΔSCF approach). Binding energies of the initial- and final-state levels are also determined by performing separate relativistic self-consistent-field (SCF) calculations for the neutral and singly ionized atom and for the neutral and doubly ionized atom, respectively.

Apart from the comparison between calculated and experimental Auger energies, a comparison of the theoretical binding energies with the experimental ones, which are determined by means of photoelectron spectroscopy and optical spectroscopy, is also presented. The considerable deviations between the experimental and theoretical binding energies clearly demonstrate the presence of electron correlation either in the initial or in the final state of the Auger decay.

II. CALCULATIONS

The calculations were carried out with the multiconfiguration Dirac-Fock code of Grant *et al.*[1,2] The computer program is fully described in the papers of Grant *et al.*[1,2] and therefore only a brief summary will be given here.

The atomic-state wave function (ASF) is presented as a linear combination of configuration-state functions (CSF). The CSF are constructed from antisymmetric products of Dirac central-field spinors and correspond to a pure *jj*-coupled state. The orbitals used to construct the ASF are determined in this paper by the average level procedure; this involves a variational calculation based on an energy functional which is the average energy of all CSF with a common value of J. Optimal level calculations, where the orbitals are optimized for a particular level, were found to be unreliable unless the corresponding large-c limit results are subtracted.[3] Because the energy expression for Breit interaction involves a very large number of small terms, this contribution is omitted in determining the orbitals, and the Hamiltonian used in the variational principle is taken to consist of a sum of single-particle Dirac Hamiltonians plus the purely Coulombic interelectron repulsion. The contributions of Breit interaction, along with other quantum-electrodynamic (QED) contributions, are added to the Hamiltonian matrix once the orbitals have been determined, and the complete matrix of Hamiltonian diagonalized to determine the corrected energy levels and ASF mixing coefficients.

Theoretical kinetic energies of the Auger transitions of Table I are predicted by single-manifold Dirac-Fock calculations. A manifold of CSF consists of all CSF mapping into the same nonrelativistic configuration. Multiconfiguration calculations, including the interactions with the nearest bound states are presented for some selected examples. All the calculations shown in Table I include the Breit contribution. The Breit energy corrections, obtained as a first-order perturbation, are presented separately for the initial- and final-state energy levels in Table II. The pure Dirac-Fock results as well as the results predicted after introducing the Breit interaction are discussed for the fine structure of the Auger transitions of Hg.

III. DISCUSSION

The experimental Auger spectra typically consist of several fine-structure components spread over a 10—20-eV energy range. Identification of the detailed lines is needed before a comparison between the experimental and theoretical energies can be made.

A complete interpretation of the fine structure of the experimental spectra is usually possible only for atoms

TABLE I. Experimental and calculated Auger and binding energies (in eV).

Element	Transition	Auger energy		Binding energy			
				Initial state		Final state	
		Experiment	Theory	Experiment	Theory	Experiment	Theory
$_{10}$Ne	$KL_{2,3}L_{2,3}(^1D_2)$	804.46[a]	806.78	870.21[b]	869.33	65.73[c]	62.55
$_{11}$Na	$KL_{2,3}L_{2,3}(^2D_{5/2})$	977.2[d]	979.12	1078.9[e]	1078.29	101.92[c]	99.17
$_{12}$Mg	$KL_{2,3}L_{2,3}(^1D_2)$	1167.0[d]	1168.92	1311.4[f]	1310.85	143.9[g]	141.93
$_{18}$Ar	$KL_{2,3}L_{2,3}(^1D_2)$	2660.5[h]	2660.78				
	$L_1L_{2,3}M_1(^3P_1)$	30.5[i]	28.04	326.0[j]	327.02	295.5[g]	298.98
	$L_3M_{2,3}M_{2,3}(^1D_2)$	203.50[a]	205.01	248.63[b]	248.18	45.13[c]	43.15
$_{19}$K	$L_3M_{2,3}M_{2,3}(^2D_{5/2})$	236.6[k]	238.16	300.5[l]	300.38	63.87[c]	62.22
$_{29}$Cu	$L_3M_{4,5}M_{4,5}(^2G_{7/2})$	900.7[m]	905.33	939.7[n]	938.88	39.05[o]	33.55
$_{30}$Zn	$L_3M_{2,3}M_{4,5}(^1F_3)$	886.7[d]	886.31	1028.9[l]	1028.56	142.2[g]	142.24
	$L_3M_{4,5}M_{4,5}(^1G_4)$	974.4[d]	978.60	1028.9[l]	1028.56	54.5[g]	49.96
$_{36}$Kr	$L_3M_{4,5}M_{4,5}(^1G_4)$	1460.4[p]	1463.72				
	$M_5N_{2,3}N_{2,3}(^1D_2)$	53.7[d]	53.85	93.8[q]	92.18	40.1[g]	38.33
$_{46}$Pd	$M_5N_{4,5}N_{4,5}(^1G_4)$	311.2[d]	313.59	341.1[n]	339.93	29.97[o]	26.34
$_{47}$Ag	$M_4N_{4,5}N_{4,5}(^2G_{7/2})$	335.8[r]	338.06	375.5[n]	374.64	39.69[o]	36.58
$_{48}$Cd	$M_5N_{4,5}N_{4,5}(^1G_4)$	361.2[d]	363.16	412.1[n]	411.39	50.82[o]	48.22
$_{49}$In	$M_5N_{4,5}N_{4,5}(^2H_{9/2})$	386.3[d]	388.24				
$_{54}$Xe	$M_5N_{4,5}N_{4,5}(^1G_4)$	520.0[d]	521.83	676.7[s]	676.49	156.7[g]	154.66
	$N_5O_{2,3}O_{2,3}(^1D_2)$	32.32[t]	33.01	67.55[t]	66.52	35.23[t]	33.51
$_{55}$Cs	$M_5N_{4,5}N_{4,5}(^2G_{9/2})$	543.9[d]	545.56	731.6[l]	732.02	187.7[g]	186.46
	$N_5O_{2,3}O_{2,3}(^2D_{5/2})$	36.3[d]	36.88				
$_{70}$Yb	$M_5N_{6,7}N_{6,7}(^1I_6)$	1494.1[u]	1495.91				
	$N_5N_{6,7}N_{6,7}(^1I_6)$	152.1[v]	158.89				
$_{79}$Au	$N_7O_{4,5}O_{4,5}(^2G_{9/2})$	54.9[d]	55.25	91.6[n]	88.76	36.89[o]	33.51
$_{80}$Hg	$N_5N_{6,7}N_{6,7}(^1I_6)$	119.3[w]	124.47	366.0[x]	368.98	246.7[g]	244.51
	$N_7O_{4,5}O_{4,5}(^1G_4)$	62.4[d]	62.80	107.06[s]	104.84	44.85[o]	42.04

[a]Obtained with the aid of Refs. 6 and 5 as discussed in the text.
[b]From Ref. 6.
[c]From Ref. 5.
[d]Unpublished results of our group based on new energy calibration.
[e]From Ref. 11.
[f]From Ref. 7.
[g]Obtained by subtracting the Auger energy from the initial-state energy.
[h]From Ref. 25.
[i]From Ref. 27.
[j]From Ref. 12.
[k]From Ref. 15, corrected to correspond the new energy calibration.
[l]From Ref. 8.
[m]From Ref. 16, corrected to correspond the new energy calibration.
[n]Obtained by adding the Auger energy and the final-state binding energy.
[o]From Ref. 4.
[p]From Ref. 26.
[q]From Ref. 13.
[r]From Ref. 17, corrected to correspond the new energy calibration.
[s]From Ref. 10.
[t]From Ref. 24.
[u]From Ref. 18, corrected to correspond the new energy calibration.
[v]From Ref. 19, corrected.
[w]From Ref. 20, corrected.
[x]From Ref. 14.

which have closed ground-state electron configuations or only one electron outside the closed shell. In the case of other open-shell atoms, the Auger transitions consist of several overlapping lines. Owing to the fairly large inherent linewidths arising from the short lifetimes of the initial-core hole states, the decomposition and identification of all individual lines is often difficult.

For the Auger transitions reported in this study, a complete interpretation of the Auger lines has been possible. The Rydberg-Ritz combination principle usually forms the starting point for the fine-structure analysis. The assignment of the structure is generally confirmed by comparing the experimental profiles with the calculated ones. In some cases, the energy levels for outer-shell double ion-

TABLE II. Breit energy contributions (in eV) to the initial- and final-state energies of the Auger transitions.

Element	Transition	Breit energy Initial state	Final state
$_{10}$Ne	$KL_{2,3}L_{2,3}(^1D_2)$	0.12	0.44
$_{11}$Na	$KL_{2,3}L_{2,3}(^2D_{5/2})$	0.18	0.61
$_{12}$Mg	$KL_{2,3}L_{2,3}(^1D_2)$	0.26	0.82
$_{18}$Ar	$KL_{2,3}L_{2,3}(^1D_2)$	1.27	3.29
	$L_3M_{2,3}M_{2,3}(^1D_2)$	3.50	3.49
$_{19}$K	$L_3M_{2,3}M_{2,3}(^2D_{5/2})$	4.20	4.33
$_{29}$Cu	$L_3M_{4,5}M_{4,5}(^2G_{7/2})$	17.58	18.46
$_{30}$Zn	$L_3M_{4,5}M_{4,5}(^1G_4)$	19.73	20.73
$_{36}$Kr	$L_3M_{4,5}M_{4,5}(^1G_4)$	36.87	38.83
	$M_5N_{2,3}N_{2,3}(^1D_2)$	38.87	38.81
$_{46}$Pd	$M_5N_{4,5}N_{4,5}(^1G_4)$	90.21	90.29
$_{47}$Ag	$M_5N_{4,5}N_{4,5}(^2G_{7/2})$	97.14	97.25
$_{48}$Cd	$M_5N_{4,5}N_{4,5}(^1G_4)$	104.23	104.58
$_{49}$In	$M_5N_{4,5}N_{4,5}(^2H_{9/2})$	112.14	112.31
$_{54}$Xe	$M_5N_{4,5}N_{4,5}(^1G_4)$	156.90	157.21
	$N_5O_{2,3}O_{2,3}(^1D_2)$	157.22	157.15
$_{55}$Cs	$M_5N_{4,5}N_{4,5}(^2G_{9/2})$	167.19	167.52
	$N_5O_{2,3}O_{2,3}(^2D_{5/2})$	167.55	167.46
$_{70}$Yb	$M_5N_{6,7}N_{6,7}(^1I_6)$	383.48	385.40
	$N_5N_{6,7}N_{6,7}(^1I_6)$	385.00	385.40
$_{79}$Au	$N_7O_{4,5}O_{4,5}(^2G_{9/2})$	590.42	590.14
$_{80}$Hg	$N_5N_{6,7}N_{6,7}(^1I_6)$	616.98	617.63
	$N_7O_{4,5}O_{4,5}(^1G_4)$	617.55	617.21

ized atoms corresponding to the final state of the Auger transitions are also observed in optical spectroscopy.[4,5] In that case the two experimental results can be compared with each other in order to improve the accuracy of the interpretation.

In this work the comparison between experiment and theory is first made on the absolute kinetic energies and then on the initial- and final-state energies and energy splittings of the Auger transitions. The intensity analysis is left outside the scope of this work.

Experimental Auger energies as well as binding energies of the initial and final states are tabulated together with the calculated values in Table I. Experimental binding energies for the initial states are obtained from photoelectron measurements[6–14] and for the final states from optical spectroscopy.[4,5] In some cases the initial-state binding energies are obtained by combining the observed Auger energies with the optical final-state energies. The experimental Auger energies (Table I) published recently by our group[15–20] are slightly corrected. This correction arises from the use of new and probably more accurate energy values for the Ar and Ne calibration lines. The adopted energy values for the Ar $L_3M_{2,3}M_{2,3}(^1D_2)$ and Ne $KL_{2,3}L_{2,3}(^1D_2)$ lines are 203.499 and 804.458 eV, respectively. The value for the Ar line is based on the accurate binding energy value of 248.629(10) eV reported by Petterson *et al.*[21] and King *et al.*[22] for the Ar L_3 level combined with the recent optical double-hole-state energy value of 45.127 eV for the $^1D_2$ state from the tables of Bashkin and Stoner[5] and corrected for the recoil energy of 0.003 eV. Analogously, the value of 804.458 eV for the main Ne Auger line is obtained by subtracting from the soft-x-ray binding energy[21] of 870.21(5) eV for the Ne K level the optical final-state energy[5] of 65.730 eV and the recoil energy of 0.022 eV. This Auger energy for Ne deviates slightly from the value of 804.557(17) eV given by Thomas and Shaw,[23] but it has the advantage that it is based on the soft-x-ray binding energy measurement and optical final-state energy similarly to the Auger energy for Ar. In addition, these nominal Auger energies are not affected by the post-collision interaction.

For the low-energy Auger spectra the calibration has been performed with the aid of Xe $N_{4,5}OO$ and Kr $M_{4,5}NN$ Auger spectra by using for the main lines the energy values given in Ref. 24. These energies are also based on optical results.

For some elements the experimental Auger energies have been taken from publications by other authors.[21,22,25–27] These values are shown in Table I as they are given in the original works, because the energy-calibration method is not known and energy correction is impossible.

The comparison between experimental and theoretical Auger energies in Table I shows a reasonably good agreement. The calculations were carried out within the single-manifold approximation. Discrepancies are thus expected to remain primarily due to the neglect of electron correlation. The computed values seem to be too high by 0–2 eV, which is clearly more than the experimental accuracy of 0.2 eV. This arises from the deviations between experiment and theory in both the initial and the final states. The deviations between the experimental and theoretical initial-state binding energies are generally smaller than 1 eV. In the case of the final state, the energies are underestimated in the theory by a few eV. The greater underestimation in the final state is a clear indication of a stronger correlation in the outer-shell doubly ionized atom than in the inner-shell singly ionized atom. The main discrepancies between calculated and measured binding energies can generally be removed by including ground-state configuration interaction and hole-state configuration interaction with the nearly bound states. Final-state correlation effects seem to be most remarkable when the outermost shell or the next inner shell is involved in the Auger transition. The agreement between experiment and theory clearly improves when the transitions begin to take place on the deeper shells of the atoms (see, e.g., the $KL_{2,3}L_{2,3}$ transitions for $10 \leq Z \leq 18$, the $L_{2,3}M_{4,5}M_{4,5}$ transitions for $29 \leq Z \leq 36$, and the $M_{4,5}N_{4,5}N_{4,5}$ for $46 \leq Z \leq 54$ in Table I).

Dirac-Fock calculations in intermediate coupling were carried out for the KLL transitions by Briancon and Desclaux.[28] Their results for the $KL_{2,3}L_{2,3}(^1D_2)$ transitions of Ne and Ar 806.9 and 2661.8 eV agree well with our results of 806.78 and 2660.78 eV, respectively.

The theoretical binding energies of the single-hole states shown in Table I agree well with the previously reported[11,29] calculations carried out within the single-configuration approximation. In the cases studied, the single-particle picture seems to reproduce the experimental initial-state binding energies reasonably well. If, however, the hole states lie very close to the threshold of Coster-Kronig continua, strong Coulomb interaction be-

tween the hole state and the continuum diminishes the hole-state energy, which, in turn, reduces the binding and Auger energies. For example, substantial shifts were found for the L_1 levels of $30 \leq Z \leq 47$, for the $M_1, M_{2,3}$ levels around $Z=36$ and for the $N_1, N_{2,3}$ levels around $Z=54$.[30,31] Interaction with the continuum in the final state of the Auger transitions due to the further decay of one or two of the final-state holes by the Coster-Kronig process may also considerably affect the energy.[32] In the present studies, however, the interaction with the continuum seems to play a minor role.

Electron-excited Auger energies are always affected by the post-collision interaction (PCI) between the receeding scattered electron and the ejected electrons, which is ignored in the calculations. In the above-mentioned determination of the energies of the calibration lines, the reference energies employed have been taken from PCI-free measurements, and the actual electron-excited reference Auger energies include some PCI shifts. Thus the PCI effects on the determined Auger energy values are at least partly cancelled. Within the approximation[33] which assumes a direct proportionality of the PCI shift to the inherent width of the core-hole state the cancellation is complete if the inherent core-hole width follows the energetically linear dependence between the corresponding values for Ar and Ne. This is roughly the case in the present studies. A fully theoretical estimation of the PCI shift is rather complicated, but the semiempirical approach[33] gives shift values of the order of 30 and 70 meV for Ar *LMM* and Ne *KLL* lines with 2500 eV excess energy. The PCI shifts for high excess energies are thus generally clearly less than 0.1 eV. The PCI shifts are hence negligible when the reasons for the discrepancies between experiment and theory are considered. In the case of Coster-Kronig transitions, especially when obtained at low impact energies, considerable PCI shifts may be present due to strong interaction between the slow electrons. One should, however, keep in mind that the effects of PCI on the observed energies are different in the cases of inner-shell ionization either by electrons or by photons.

The Breit and QED contributions are found to be of minor importance in the calculated absolute Auger energy values in most cases studied in this work. This is because their effect is of the same magnitude both in the initial and in the final states and is thus canceled when the Auger energies are obtained as the energy difference. The contributions of the Breit interaction to the total energies of the singly ionized initial and doubly ionized final states of the Auger transitions are given in Table II. The Breit energy corrections in passing from the single to the double hole states seem to be almost equal for the M and N Auger transitions, but for the L transitions they increase slightly and for the K transitions even considerably along with an increasing Z. Neglect of the Breit contribution may result in errors of the order of few eV in the *KLL* Auger energies in passing to the medium Z values.

As the next step we consider the energy splitting of the Auger spectra. The $KL_{2,3}L_{2,3}$ spectrum of Mg ($Z=12$), the $M_{4,5}N_{4,5}N_{4,5}$ spectrum of Cd ($Z=48$), and the $N_{6,7}O_{4,5}O_{4,5}$ spectrum of Hg ($Z=80$) are presented as examples, but the same trend is also observed for the other spectra. For these elements the energy-level structure of the final state is also known optically, and an accurate interpretation of the lines has thus been possible. Figures 1, 2, and 3 show the calculated and experimental energy-level structures of the $2p^4 3s^2$, $4d^8 5s^2$, and $5d^8 6s^2$ configurations of Mg, Cd, and Hg, respectively. The single-manifold results as well as the results obtained after introducing the interaction between the nearest two-hole configurations of the same symmetry are depicted.

An inspection of Figs. 1–3 shows the common tendency (see also Table I) that the experimental final-state energies are higher than the calculated ones. Furthermore, the calculated energy splitting appears to be larger than the experimental one, especially at lower Z values. The range of the calculated splitting decreases compared with the experimental one along with an increasing Z, and in this respect the agreement improves in passing to heavier elements, e.g., Hg ($Z=80$). This is due to the fact that for heavy elements the correlation effect becomes less important compared with the relativistic effects, which are treated more accurately in the computations. The effect of configuration interaction is most remarkable for the $J=0$ states. Only the two-hole configurations $2s^{-2}$, $2p^{-2}$, $2s^{-1}3s^{-1}$, and $3s^{-2}$ are mixed in the case of Mg, whereas, in addition to the corresponding configurations, the configurations with holes in the d orbital also interact with each other in the case of Cd and Hg. The distance between the $^1S_0$ and the other levels is clearly improved, but the detailed splittings between the levels are not too well reproduced by the multiconfiguration approach. In

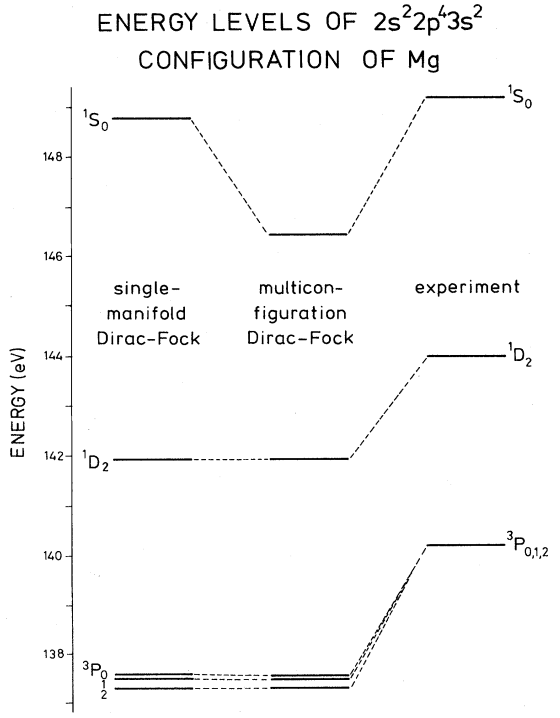

FIG. 1. Energy levels of the $2s^2 2p^4 3s^2$ configuration of Mg calculated by the single-manifold and multiconfiguration Dirac-Fock approach compared with experiment. Interaction between the configurations $2s^0 2p^6 3s^2$, $2s^1 2p^6 3s^1$, and $2s^2 2p^4 3s^0$ is taken into account.

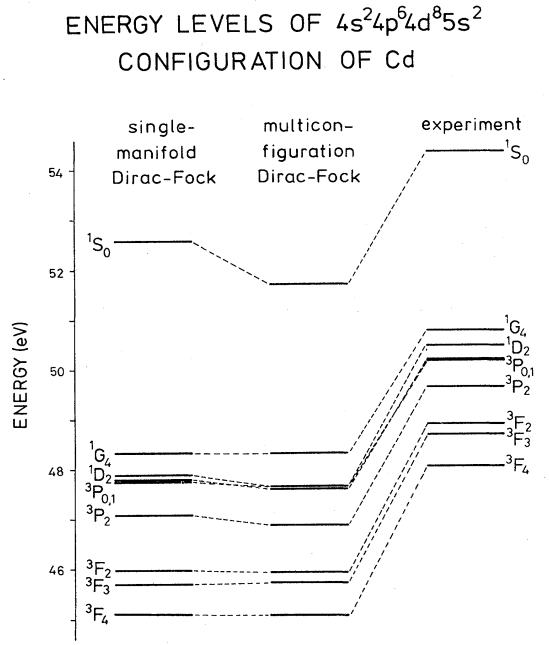

FIG. 2. Energy levels of the $4s^24p^64d^85s^2$ configuration of Cd predicted by the single-manifold and multiconfiguration Dirac-Fock calculations compared with experiment. Interaction between the two-hole configurations $4s^04p^64d^{10}5s^2$, $4s^24p^44d^{10}5s^2$, $4s^14p^64d^95s^2$, $4s^24p^64d^85s^2$, $4s^24p^64d^{10}5s^0$, $4s^14p^64d^{10}5s^1$, and $4s^24p^64d^95s^1$ is taken into account.

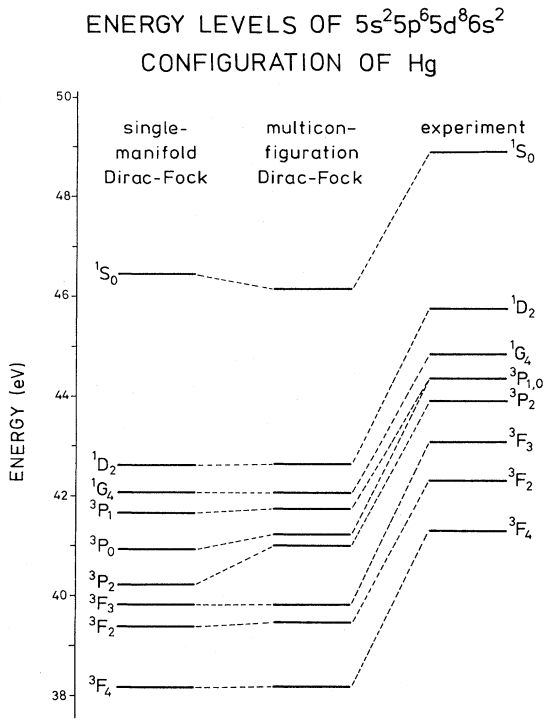

FIG. 3. Energy levels of the $5s^25p^65d^86s^2$ configuration of Hg obtained from the single-manifold and multiconfiguration Dirac-Fock calculations and from experiment. Interaction between the nearest two-hole states of the same symmetry is taken into account.

fact, it is clear that in order to arrive at a complete description of the energy-level structure, it is necessary to include the interaction with the continuum as well as the other weaker interactions.

The influence of the Breit interaction on the final-state energy spiltting is found to be of minor importance for all the studied transitions. As an example, the total and relative energies of the levels of the $4d^85s^2$ configuration of Hg are tabulated after and before introducing the Breit interaction and the other QED corrections (Table III). In some cases (e.g., the $L_{2,3}M_{4,5}M_{4,5}$ transitions of Kr) the positions of the two final-state energy levels are changed after the Breit energy correction, but due to a very small energy separation of the levels (<0.1 eV) this does not cause any remarkable effect in the profile of the spectrum.

In the case of the initial-state splitting, the Breit energy correction, being of the order of 0.5 eV, improves the agreement between experiment and theory. The Dirac-Fock calculations, after an introduction of the Breit interaction, appear to reproduce the observed splitting between the initial states with $j=l-\frac{1}{2}$ and $j=l+\frac{1}{2}$ very well in the case of the transitions now studied, the deviations from experiment being within 0.01 eV.

A comparison between relativistic and nonrelativistic intermediate-coupling calculations for the final-state energy splitting of the studied Auger spectra shows very small deviations between the two estimates. This is demonstrated in the case of the $M_{4,5}N_{4,5}N_{4,5}$ spectrum of Cd in

TABLE III. Total and relative energies (in eV) of the levels of the $5d^86s^2$ configuration of Hg predicted by the single-manifold Dirac-Fock calculations.

Level	Zero-order energy Total	Zero-order energy Relative	Zero + Breit energy Total	Zero + Breit energy Relative	Total energy with Breit and QED corrections
$^3F_4$	534 767.266	3.924	534 149.970	3.881	533 779.207
$^3F_2$	534 766.058	2.716	534 148.763	2.674	533 778.000
$^3F_3$	534 765.566	2.224	534 148.315	2.226	533 777.552
$^3P_2$	534 764.471	1.129	534 147.223	1.134	533 776.460
$^3P_0$	534 764.206	0.864	534 146.924	0.835	533 776.161
$^3P_1$	534 763.744	0.402	534 146.491	0.402	533 775.728
$^1G_4$	534 763.342	0.000	534 146.089	0.000	533 775.326
$^1D_2$	534 762.745	−0.597	534 145.533	−0.556	533 774.770
$^1S_0$	534 758.927	−4.415	534 141.701	−4.388	533 770.938

TABLE IV. Relative energies (in eV) of the levels of the $4d^8 5s^2$ configuration of Cd predicted by the multiconfiguration Dirac-Fock (MCDF) calculations compared with conventional nonrelativistic intermediate coupling energies and with experiment.

	Relativistic		Nonrelativistic		
Level	Single manifold	Multi-configuration	Single configuration	Configuration interaction	Experiment
$^3F_4$	3.25	3.24	3.29	3.29	2.73
$^3F_3$	2.64	2.60	2.67	2.67	2.01
$^3F_2$	2.37	2.39	2.39	2.44	1.94
$^3P_2$	1.25	1.43	1.26	1.49	1.10
$^3P_0$	0.54	0.68	0.55	0.77	0.53
$^3P_1$	0.57	0.72	0.59	0.78	0.44
$^1D_2$	0.45	0.69	0.45	0.69	0.31
$^1G_4$	0.00	0.00	0.00	0.00	0.00
$^1S_0$	−4.25	−3.42	−4.29	−3.33	−3.65

Table IV. The Hartree-Fock program of Froese Fischer was used to obtain the numerical values of Slater integrals and spin-orbit parameters for the nonrelativistic intermediate-coupling energy matrix.[34] The interaction between the final-state configurations $4s^{-2}$, $4p^{-2}$, $4s^{-1}4d^{-1}$, $4d^{-2}$, $5s^{-2}$, $4s^{-1}5s^{-1}$, and $4d^{-1}5s^{-1}$ was treated by using the multiconfiguration procedure in the relativistic computations, but the first-order perturbation (the configuration interaction approximation) in the nonrelativistic ones. In the relativistic case the spin-orbit interaction is included in the variational calculation, since the associated operator belongs to the Dirac one-electron Hamiltonian. In the nonrelativistic analog the intermediate coupling is treated as a kind of limited configuration interaction due to the spin-orbit interaction. Regardless of the different computational methods, good agreement between the two results is found. This indicates the usefulness of the simple nonrelativistic intermediate-coupling scheme in reproducing the final-state energy splitting. The finding is not surprising in the respect that the energy corrections arising from the Breit Hamiltonian are found to be of minor importance, and precisely these corrections due to the spin-other-orbit, orbit-orbit, and spin-spin perturbations are competely omitted in the nonrelativistic intermediate-coupling approach.

IV. CONCLUSIONS

The Dirac-Fock calculations are found to reproduce the energies of the Auger transitions reasonably well. The Auger energies are usually overestimated in the theory by 0—2 eV due to strong electron correlation in the doubly ionized final state. Electron correlation, which may randomly play a dominant role, may also cause discrepancies up to 5—6 eV between experiment and theory.[30,31] The agreement with experiment in reproducing the fine structure of the spectra due to the final-state splitting is found to increase along with an increasing atomic number. The role of the Breit interaction appears to be of minor importance in the Auger processes studied. The Coster-Kronig transitions may be more sensitive to the effects of the interaction with the continuum[30] and the Breit interaction.[35]

ACKNOWLEDGMENTS

This work has been supported by the Finnish Academy for Science.

[1]I. P. Grant, B. J. McKenzie, and P. H. Norrington, Comput. Phys. Commun. 21, 207 (1980).
[2]B. J. McKenzie, I. P. Grant, and P. H. Norrington, Comput. Phys. Commun. 21, 233 (1980).
[3]N. C. Pyper, J. Phys. B 16, L211 (1983).
[4]C. E. Moore, *Atomic Energy Levels, National Stand. Ref. Data Ser. 467* (National Bureau of Standards, Washington, D.C., 1971), Vols. 1—3.
[5]S. Bashkin and J. O. Stoner, Jr., *Atomic Energy-Level and Grotrian Diagrams* (North-Holland, Amsterdam, 1978), Vols. 1 and 2.
[6]L. Petterson, J. Nordgren, L. Selander, C. Nordling, and K. Siegbahn, J. Electron Spectrosc. Relat. Phenom. 27, 29 (1982).
[7]M. S. Banna, A. R. Slaughter, R. D. Mathews, R. J. Key, and S. M. Ballina, Chem. Phys. Lett. 92, 122 (1982).
[8]R. J. Key, M. S. Banna, and S. C. Ewing, J. Electron Spectrosc. Relat. Phenom. 24, 173 (1981).
[9]S. Svensson, N. Mårtensson, E. Basilier, P. Å. Malmquist, U. Gelius, and K. Siegbahn, Phys. Scr. 14, 141 (1976).
[10]S. Svensson, N. Mårtensson, E. Basilier, P. Å. Malmquist, U. Gelius, and K. Siegbahn, J. Electron Spectrosc. Relat. Phenom. 9, 51 (1976).
[11]M. S. Banna, R. J. Key, and C. S. Ewing, J. Electron Spectrosc. Relat. Phenom. 26, 259 (1982).
[12]J. Nordgren, H. Ågren, C. Nordling, and K. Siegbahn, Phys. Scr. 19, 5 (1979).
[13]K. Codling and R. P. Madden, Phys. Rev. Lett. 12, 106 (1964).
[14]K. Siegbahn, J. Electron Spectrosc. Relat. Phenom. 5, 3 (1974).
[15]S. Aksela, M. Kellokumpu, H. Aksela, and J. Väyrynen, Phys. Rev. A 23, 2374 (1981).
[16]S. Aksela and J. Sivonen, Phys. Rev. A 25, 1243 (1982).
[17]J. Väyrynen, S. Aksela, M. Kellokumpu, and H. Aksela, Phys. Rev. A 22, 1610 (1980).
[18]S. Aksela and H. Aksela, Phys. Rev. A 27, 3129 (1983).
[19]I. Chorkendorff, J. Onsgaard, H. Aksela, and S. Aksela, Phys.

Rev. B 27, 945 (1983).
[20]H. Aksela and S. Aksela, J. Phys. B 16, 1531 (1983).
[21]L. Petterson, J. Nordgren, L. Selander, C. Nordling, and K. Siegbahn, J. Electron Spectrosc. Relat. Phenom. 27, 29 (1982).
[22]G. C. King, M. Trone, F. H. Read, and R. C. Brandford, J. Phys. B 10, 2479 (1977).
[23]T. D. Thomas and R. W. Shaw, Jr., J. Electron Spectrosc. Relat. Phenom. 5, 1081 (1974).
[24]J. E. Hansen and W. Persson, Phys. Rev. A 20, 364 (1979).
[25]L. Asplund, P. Blomster, H. Siegbahn, and K. Siegbahn, Phys. Scr. 16, 268 (1977).
[26]L. O. Werme, T. Beckmark, and K. Siegbahn, Phys. Scr. 6, 141 (1972).
[27]W. Mehlhorn, Z. Phys. 208, 1 (1968).
[28]Ch. Briancon and J. P. Desclaux, Phys. Rev. A 13, 2157 (1976).
[29]K.-N. Huang, M. Aoyagi, M. H. Chen, B. Crasemann, and H. Mark, At. Data Nucl. Data Tables 18, 243 (1976); 26, 561 (1981).
[30]M. H. Chen, B. Crasemann, and H. Mark, Phys. Rev. A 24, 1158 (1981).
[31]G. Wendin and M. Ohno, Phys. Scr. 14, 148 (1976); 16, 299 (1977).
[32]M. Ohno, and J.-M. Mariot, J. Phys. C 14, L1133 (1981).
[33]S. Hedman, K. Helenelund, L. Asplund, U. Gelius, and K. Siegbahn, J. Phys. B 15, L799 (1982).
[34]H. Aksela and S. Aksela, J. Phys. B 7, 1262 (1974).
[35]M. H. Chen, B. Crasemann, and H. Mark, Phys. Rev. A 25, 391 (1982).